DOI: 10.1002/chem.200901270

High-Affinity Inhibitors of tRNA-Guanine Transglycosylase Replacing the Function of a Structural Water Cluster

Philipp C. Kohler,[a] Tina Ritschel,[b] W. Bernd Schweizer,[a] Gerhard Klebe,[b] and François Diederich*[a]

Abstract: The tRNA-modifying enzyme tRNA–guanine transglycosylase (TGT) is essential for the pathogenic mechanism of *Shigella flexneri*, the causing agent of the bacterial diarrheal disease shigellosis. Herein, the synthesis of a new class of rationally designed 6-amino-imidazo[4,5-*g*]quinazolin-8(7*H*)-one- (*lin*-benzoguanine) based inhibitors of TGT are reported. In order to accommodate a small hydrophobic crevice opening near the binding site of ribose-34, 2-aminoethyl substituents were introduced in position 4 of the heterocyclic scaffold. For this purpose, a synthetic sequence consisting of iodination, Suzuki cross-coupling, hydroboration, Mitsunobu reaction, and Gabriel synthesis was employed, furnishing a primary amine that served as a common intermediate for the preparation of a series of derivatives. The resulting ligands displayed very low inhibition constants, down to $K_i = 2$ nM. Substantial additional inhibitory potency is gained by interaction of terminal lipophilic groups attached to the substituent at position 4 with the hydrophobic crevice shaped by Val45 and Leu68. At the same time, the secondary ammonium center in the substituent displaces a cluster of water molecules, solvating the catalytic residues Asp102 and Asp280, without loss in binding affinity. In addition, a synthetic intermediate with an unusual 3,6,7,8,9,10-hexahydroimidazo[4,5-*g*]-[1,3]benzodiazepine core, as confirmed by X-ray analysis, is reported.

Keywords: antibiotics · drug design · glycosylases · inhibitors · shigellosis

Introduction

The tRNA modifying enzyme tRNA–guanine transglycosylase (TGT, EC 2.4.2.29) has been recognized as a potential target for the design of new drugs against shigellosis,[1] a bacterial diarrheal disease causing approximately 1.1 million fatalities each year.[2] Eukaryotic TGT catalyzes the exchange of guanine-34 by queuine (Q, 7-{[(4,5-*cis*-dihydroxy-2-cyclopenten-1-yl)amino]methyl}-7-deazaguanine), while prokaryotic TGT mediates the exchange of guanine by the Q-precursor preQ$_1$ (7-aminomethyl-7-deazaguanine).[3] In view of the distinctively different substrates, selectivity for the causing agent *Shigella flexneri* should be achievable. We have previously introduced 6-amino-imidazo[4,5-*g*]quinazolin-8(7*H*)-one (*lin*-benzoguanine)[4] as a promising scaffold for the design of TGT inhibitors.[5,6] We subsequently demonstrated the large potential of this heterotricyclic scaffold with a series of inhibitors featuring amino substituents in position 2, which reach into the spacious ribose-33 pocket (for the numbering see Table 1).[7,8] Some of these ligands afforded inhibitory constants K_i down to the single-digit nanomolar range.[7,8] Here, we report a new series of highly active ligands featuring a substituent in position 4 to address the hydrophobic surface depression shaped by Val45 and Leu68 near the ribose-34 site without paying, as with previous ligands,[5,6] a large energetic penalty for replacing a consensus water cluster solvating the two catalytic Asp side chains (Asp102 and Asp280) of the enzyme.

[a] P. C. Kohler, Dr. W. B. Schweizer, Prof. Dr. F. Diederich
Laboratorium für Organische Chemie, ETH Zürich
Hönggerberg, HCI, 8093 Zürich (Switzerland)
Fax: (+41) 44-632-1109
E-mail: diederich@org.chem.ethz.ch

[b] T. Ritschel, Prof. Dr. G. Klebe
Institut für Pharmazeutische Chemie
Philipps-Universität Marburg, Marbacher Weg 6
35032 Marburg (Germany)
Fax: (+49) 6421-282-8994

Supporting information for this article is available on the WWW under http://dx.doi.org/10.1002/chem.200901270.

Results and Discussion

Replacement of structural water: The replacement of structural water near polar enzyme functionalities by ligands re-

Table 1. Previously synthesized *lin*-benzoguanine inhibitors substituted in position 4 and their respective inhibition constants for *Z. mobilis* TGT.[5]

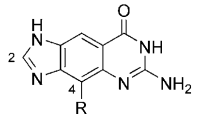

Compound	R	K_i/nM
1	H	4100 ± 1000[a]
2	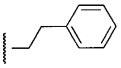	1000 ± 300
3	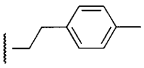	6900 ± 1700
4	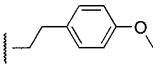	3700 ± 900

[a] Competitive inhibition constant K_{ic} (uncompetitive inhibition constant $K_{iu} = 7900$ nM). For all other compounds presented in this work, uncompetitive inhibition is negligible.

mains a major challenge in rational drug design. Until recently, such water present in binding sites was usually neglected in the design of ligands, as it was conceptually difficult to handle. Generally, the entropic benefit of releasing trapped water into the bulk phase was deemed sufficient for justifying displacement. When structural water molecules are required for stabilizing and solvating hydrophilic enzyme functionalities, however, this approach becomes problematic.[9] Desolvation of such residues can lead to severe enthalpic penalties that are hard to identify and nontrivial to overcome. An early example where the importance of fixed water molecules was recognized is that of the L-arabinose binding protein, which is selective for L-arabinose over D-fucose because of unfavorable interactions of bound water molecules with the D-fucose methyl group. The water can be replaced by a CH_2OH group of D-galactose, resulting in strong binding.[10] In the case of HIV-1 protease, fixed water was successfully replaced by an inhibitor in which the water molecule was mimicked by a cyclic urea moiety.[11] For the oligopeptide-binding protein OppA, it has been shown that the water content of the binding site can change according to the nature of the bound tripeptide Lys-X-Lys, where X is variable, and that OppA is thus able to accommodate different side chains of X of varying size and polarity.[12] Recently, several attempts were made to classify crystal water in protein structures as "replaceable" or "non-replaceable" by computational means.[13–15]

From a thermodynamic point of view, the binding free enthalpy associated with binding of a ligand into a water-containing pocket can be split into an enthalpic and an entropic part, both of which have contributions originating from the ligand, the protein, and from the released water.[9] We can distinguish the cases of apolar and polar pockets. In the former case, the contribution from the water release is both enthalpically and entropically favorable. Inside the pocket, some water molecules are unable to form four virtually unperturbed hydrogen bonds, experiencing at the same time a highly dynamic disorder of donor and acceptor functionality as present in an extensive water network, which is possible in the bulk solution; therefore their release has a negative enthalpy term. Entropically, the gain in degrees of freedom associated with this release is favorable. In the case of a polar binding pocket, the release of structural water is still associated with a favorable entropy term, as the orientation of the water molecules will be constrained by the environment, but here the desolvation of polar protein functionalities has an enthalpic cost. The desolvation free energy is close to zero if the enthalpic cost is ≈ 5 kcal mol^{-1}, about the enthalpy of a hydrogen bond.[16,17] If the bound water provides even more stabilization to the polar pocket or contributes to a residual solvation of polar functional groups, the overall release can become strongly unfavorable. In ligand design, this must of course be counterbalanced by a free enthalpy gain provided by additional ligand-protein interactions - in other words, replacement of the lost protein–water hydrogen bond(s) by protein–ligand interactions.

Preliminary work: The TGT active site exhibits a hydrophobic patch formed by Val45 and Leu68, where the phosphate, linking ribose-34 to ribose-35, in bound tRNA is located. In previous work, *lin*-benzoguanine- (**1**) derived inhibitors bearing substituents in position 4 (**2–4**) were synthesized in order to gain hydrophobic interactions with this patch. The synthesis relied on Sonogashira coupling of phenylacetylenes with a 4-iodobenzimidazole as precursor to the *lin*-benzoguanine scaffold and subsequent reduction of the triple bond.[5] When the inhibition constants were compared with that of the unsubstituted scaffold **1**, no significant improvement in binding affinity was seen, although crystal structures of enzyme–ligand complexes showed binding of the substituents in the ribose-34 pocket (Table 1).

In another study, we carefully analyzed the enzyme's active site.[19] This computation and structure-based approach revealed a well-defined water cluster located between the two catalytic aspartates Asp102 and Asp280. A ReliBase+[18] search of all known TGT crystal structures was performed to derive a set of consensus water positions.[19] A superposition of the crystal structure of inhibitor **2** in the active site with this consensus water cluster (Figure 1) reveals an explanation for the relatively poor affinities of inhibitors **2–4**: The water cluster is essential for the solvation of the negatively charged residues of Asp102 and Asp280.[6,19] Upon binding of an appropriately substituted inhibitor, the substituent attached to address the hydrophobic surface depression to accommodate ribose-34 displaces the water molecules to varying extent, leaving the aspartates "naked". This results in Coulomb repulsion of the two most likely negatively charged residues as well as unfavorable $CO_2^- \cdots CH_2$ interactions with the apolar substituent, which cause the side chain to distribute over two conformations. The concomitant enthalpic cost is only partially compensated by the favorable interactions with the ribose-34 hydrophobic surface and the entropic benefit[16] resulting from the release of water molecules into the bulk solvent. Thus,

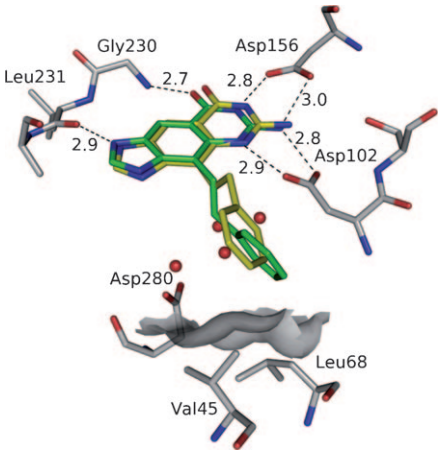

Figure 1. Crystal structure of inhibitor **2** (yellow: "up" conformer; green: "down" conformer) in the TGT active site (grey), overlaid with the consensus water cluster (red) located between Asp102 and Asp280. Dashed lines represent hydrogen bonds to the "down" conformer. The residues Val45 and Leu68 form a hydrophobic surface (shown) that is occupied by the phenyl substituent of **2**. The phenethyl moiety of **2** crosses the water cluster, thereby expelling the water molecules from the active site. Atom distances in Å. PDB code 1Y5V.[5]

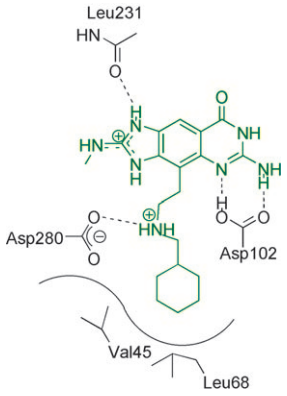

Figure 2. Predicted binding mode of the designed inhibitor **5** (green) in the TGT active site (black). The protonated amino linker undergoes a hydrogen bond to Asp280, while the hydrophobic cyclohexyl ring occupies the hydrophobic surface formed by Val45 and Leu68.

the overall binding affinity is left unchanged or somewhat reduced when compared to the unsubstituted parent scaffold, which leaves the cluster of water molecules unperturbed.

Ligand design: The rational design of the new ligands, described in detail elsewhere,[19] was based on a DrugScore^{CSD} HotSpot analysis, docking studies using GOLD,[13] and modeling with the program MOLOC;[20] and has been rigorously validated by extensive crystal structure determinations.[19] We reasoned that side chains must be able to take over the function of the expelled water molecules and pick up the H-bond network with remaining water molecules and the aspartate side chains. At the same time, they should bear a hydrophobic moiety capable of undergoing favorable hydrophobic interactions with the ribose-34 surface. Secondary amines were deemed especially suitable as polar linkers because they were assumed to be protonated in the TGT active site, thus forming a strong ionic hydrogen bond to Asp280. As apolar substituents, small hydrocarbon rings, such as cyclohexane, were chosen. Previous work had shown that substitution of the *lin*-benzoguanine scaffold with a 2-methylamino group is highly favorable because it raises the pK_a of the fused imidazole ring by about one unit. The protonation of the aminoimidazole moiety enables the formation of a charge-assisted hydrogen bond to the Leu231 backbone carbonyl.[7,8] Therefore, the 2-methylamino group was also incorporated in the designed ligands, resulting in *lin*-benzoguanine **5** (Figure 2).[19]

Synthesis: The previously reported synthesis of 4-substituted *lin*-benzoguanines employed Sonogashira cross-couplings of phenylacetylenes with a 4-iodobenzimidazole to introduce the side chain. The triple bond was then reduced to the ethanediyl linker.[5] *N*-Alkynylamides (ynamides) can be prepared from the corresponding secondary amides and bromoacetylenes using a copper(II) catalyzed cross-coupling reaction.[21] Attempts were made to couple such alkynes to an iodinated benzimidazole and subsequently hydrogenate the triple bond, but this strategy was found to be impractical and only seemed to work with alkynylsulfonamides, which are hard to hydrolyze to the unprotected amines. To avoid these problems, a different reaction sequence was chosen.

The synthesis started from commercially available benzimidazole-5-carboxylic acid (**6**), which was esterified, nitrated, and *N*-protected to furnish a mixture of isomers **7a** and **7b**. Bromination of isomer **7a** in position 2, furnishing intermediate **8**,[7] followed by S_NAr substitution with methylamine, delivered 2-(methylamino)benzimidazole (**9**). After reduction of the nitro group, iodination of 5-aminobenzimidazole **10** occurred exclusively in position 4 to give benzimidazole **11** in excellent yield. Suzuki cross-coupling with 4,4,5,5-tetramethyl-2-vinyl-1,3,2-dioxaborolane furnished 4-vinylbenzimidazole **12**. This styrene derivative could be converted to alcohol **13** by hydroboration with 9-BBN, followed by oxidative workup (Scheme 1).

In a first attempt to synthesize a secondary amine bearing a hydrophobic substituent, alcohol **13** was tosylated and subsequently substituted with (cyclohexylmethyl)amine. Yields in this procedure were unsatisfactory because of side products resulting from *N*-tosylation of the exocyclic NH_2 group of the *lin*-benzoguanine or elimination instead of substitution. Still, it was possible to cyclize benzimidazole **14** with chloroformamidinium chloride under very harsh reaction conditions with concomitant *N*-deprotection to yield the desired inhibitor **5** (Scheme 2).

Because the tosylation–substitution sequence (Scheme 2) was thought unsatisfactory, a more reliable synthetic pathway was searched for. Cyclization of alcohol **13** with chloroformamidinium chloride gave access to *lin*-benzoguanine **15**. Alternatively, a Mitsunobu reaction of alcohol **13**, followed by cleavage of phthalimide **16** with hydrazine, furnished the primary amine **17**. Cyclization with chloroformamidinium

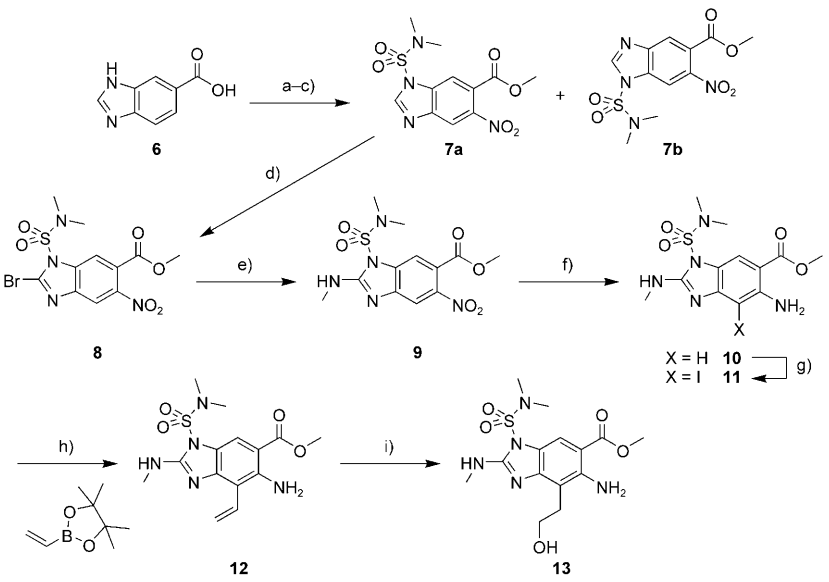

Scheme 1. Synthesis of alcohol **13**. a) $SOCl_2$, MeOH, 50°C; 97%. b) HNO_3, H_2SO_4, 50°C; 76%. c) Me_2NSO_2Cl, Et_3N, toluene, reflux; 35% **4a**, 29% **4b**. d) 1) LHMDS, THF, −78°C; 2) CBr_4, THF, −78 → 22°C; 56%. e) $MeNH_2$, EtOH, 0°C; 91%. f) Zn, AcOH, H_2O, 22°C; 94%. g) I_2, $NaHCO_3$, CH_2Cl_2, H_2O, 22°C; 98%. h) $[PdCl_2(PPh_3)_2]$, Et_3N, DME, H_2O, 80°C; 87%. i) 1) 9-BBN, THF, 22°C; 2) H_2O_2, NaOH, H_2O, 0 → 22°C; 70%. LHMDS = lithium hexamethyldisilazide; DME = 1,2-dimethoxyethane; 9-BBN = 9-borabicyclo[3.3.1]nonane.

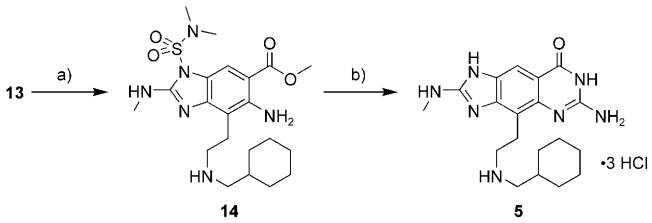

Scheme 2. First-approach to the synthesis of inhibitor **5**. a) 1) *p*TsCl, Et_3N, DMAP, CH_2Cl_2, 0°C; 2) (cyclohexyl)methylamine, CH_2Cl_2, 0 → 22°C; 38%. b) Chloroformamidinium chloride, dimethyl sulfone, 150°C; 54%. *p*TsCl = *para*-toluenesulfonyl chloride; DMAP = 4-(dimethylamino)pyridine.

chloride yielded *lin*-benzoguanine **18**, while reductive amination with appropriate aldehydes gave access to the secondary amines **14** and **19**–**22**, and, after cyclization, to *lin*-benzoguanines **5** and **23**–**26**, respectively. The cyclization yields were somewhat lower for the benzylic amines **25** and **26** due to partial debenzylation under the reaction conditions. This synthetic sequence is less prone to side reactions than the first approach. Rather, it seems to be applicable to a large variety of aldehydes RCHO, giving easy access to a broad range of substituents (Scheme 3).

For the synthesis of the control compound **27** with an *N*-methylaminoethyl substituent, a benzyl protecting group had to be introduced to prevent double methylation of the primary amine **17**. When benzylated intermediate **21** was subjected to mild Eschweiler–Clarke-type conditions, tetrahydro-1,3-benzodiazepine **28** was obtained exclusively. Few examples[22–25] are known of this unusual structure that was first reported by DeStevens and Dughi.[26] X-ray structure analysis confirmed the presence of the seven-membered cyclic aminal (Figure 3). Subsequent reduction of the crude intermediate with $NaBH(OAc)_3$ furnished the desired tertiary amine **29** as a single product. Hydrogenolysis provided methylamine **30**, and subsequent cyclization gave *lin*-benzoguanine **27** (Scheme 4).

Control compound **31** was synthesized by acylation of amine **17**, followed by cyclization of the resulting amide **32**. The 4-phenylbutyl substituent of *lin*-benzoguanine **33** was introduced by Sonogashira cross-coupling of aryl iodide **11** with 4-phenyl-1-butyne to furnish alkyne **34**. Hydrogenation of the triple bond to the alkyl derivative **35** required repeated

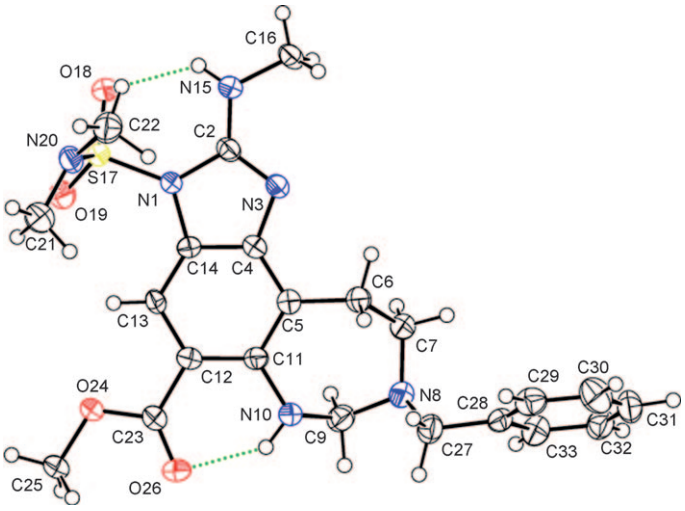

Figure 3. Molecular structure of **28** (ORTEP plot), arbitrary numbering. Atomic displacement parameters obtained at 203 K are drawn at the 50% probability level. The two NH groups form intramolecular H-bonds (green dotted; N10-H···O26: 1.97 Å, N15-H···O18 2.10 Å).

addition of catalyst, presumably due to poisoning by the substrate (total catalyst load of 28 mol%). Cyclization with chloroformamidinium chloride afforded the tricycle **33** (Scheme 5).

Biological activity: The synthesized inhibitors were subjected to kinetic measurements with the enzyme, as described in the literature.[5,7,8] Simple substitution of the parent scaffold 2-methylamino-*lin*-benzoguanine (**36**)[7,8] with a 4-phenylbu-

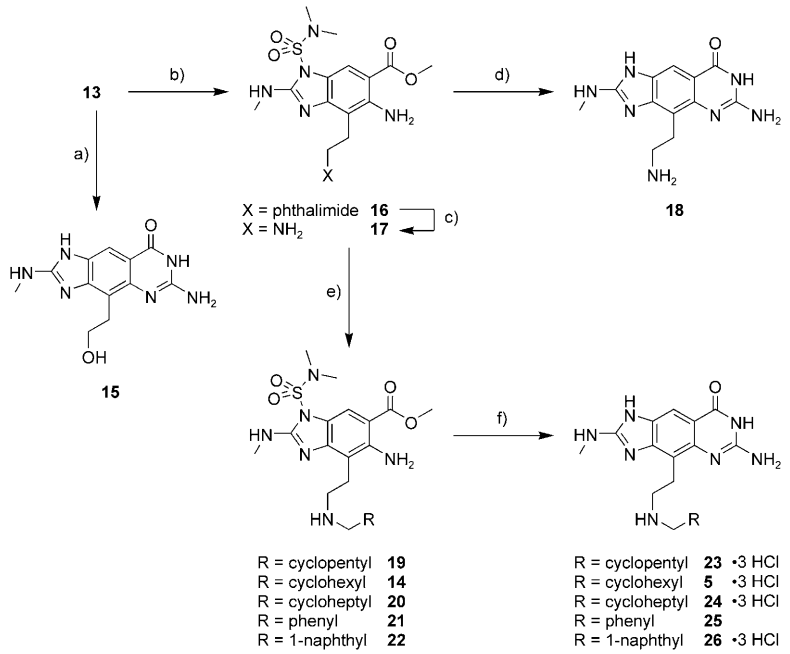

Scheme 3. Synthesis of inhibitors **5**, **15**, **18**, and **23**–**26**. a) Chloroformamidinium chloride, dimethyl sulfone, 150 °C; 65 %. b) Phthalimide, PPh_3, DIAD, CH_2Cl_2, 22 °C; 85 %. c) $H_2NNH_2 \cdot H_2O$, CH_2Cl_2/MeOH, 22 °C; 96 %. d) Chloroformamidinium chloride, dimethyl sulfone, 150 °C; 68 %. e) RCHO, $NaBH(OAc)_3$, CH_2Cl_2, 22 °C; 60 % **19**, 61 % **14**, 55 % **20**, 71 % **21**, 63 % **22**. f) Chloroformamidinium chloride, dimethyl sulfone, 150 °C; 67 % **23**, 54 % **5**, 76 % **24**, 26 % **25**, 41 % **26**. DIAD = diisopropyl azodicarboxylate.

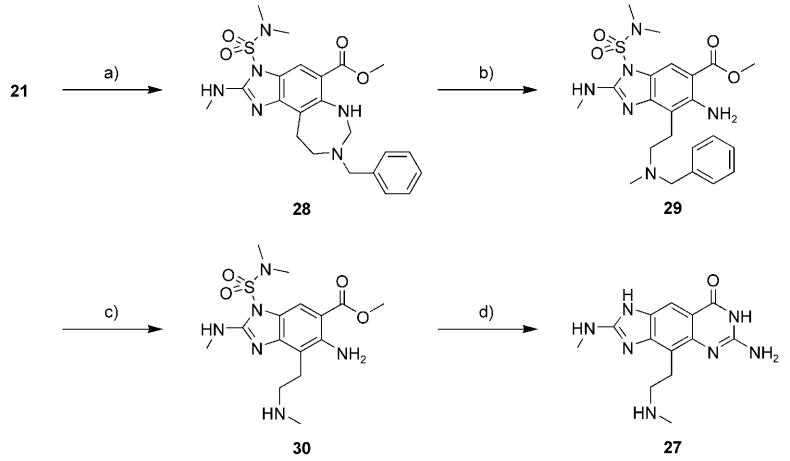

Scheme 4. Synthesis of inhibitor **27**. a) CH_2O, HCO_2H, CH_2Cl_2/H_2O, 0 → 22 °C. b) $NaBH(OAc)_3$, 1,2-dichloroethane, reflux; 83 % over two steps. c) 1 bar H_2, Pd/C, THF, 22 °C; 87 %. d) Chloroformamidinium chloride, dimethyl sulfone, 150 °C; 60 %.

tyl residue (**33**) results in a loss in affinity due to repulsive interactions between the alkyl chain and the negatively charged Asp102 and Asp280 side chains and due to the expulsion of the solvating water molecules. In this case, the repelled water cluster is obviously not properly replaced. Inhibitor **15** bearing a 2-hydroxyethyl group in position 4 loses a factor of 1.7 in binding affinity compared to the parent scaffold **36**. The conserved binding mode of compound **15** could be confirmed by crystal structure analysis described elsewhere.[19] Apparently, the uncharged hydroxy group cannot fully replace the expelled water molecules in terms of hydrogen bonding to the Asp side chains and residual water molecules. This goal is apparently achieved by the amino- and methylamino-substituted compounds **18** and **27**, which show the same or a slightly improved affinity, respectively. An amide linker (**31**) leads again to a strong loss in binding potency because the amide bond lacks a positive charge and seems to be too rigid and unable to undergo the necessary hydrogen bonds. Furthermore, inadequate desolvation of the amide bond upon transfer from the bulk water environment to the protein binding site is detrimental to high affinity binding. Although benzylamine **25** bears a hydrophobic phenyl substituent on the amino group, it displays the same K_i value as control compound **27**. In the case of naphthalene **26**, there is even a loss in affinity. It seems that aromatic substituents are too rigid to align optimally to the hydrophobic surface crevice. The *lin*-benzoguanines **23**, **5**, and **24** with alicyclic substituents on the secondary amine linker, on the other hand, display strong inhibitors of TGT in the low nanomolar range. The strongest inhibitor **23** (2 nM) exhibits a ~30-fold increase in binding strength compared to the unsubstituted scaffold **36**, confirming the formation of favorable hydrophobic interactions with the apolar surface near ribose-34 (Table 2).[19]

These results, together with the previously reported ones (Table 1),[5] are strong evidence for the validity of our design hypothesis. The water cluster located between Asp102 and Asp280 can be successfully replaced by substituents bearing a polar, H-bond-forming functionality in the appropriate position. The protonated secondary ammonium ions **18** and **27** succeed in replacing the function of the expelled water molecules by forming strong ionic H-bonds to Asp280 and participating in the H-bonding network of the remaining water

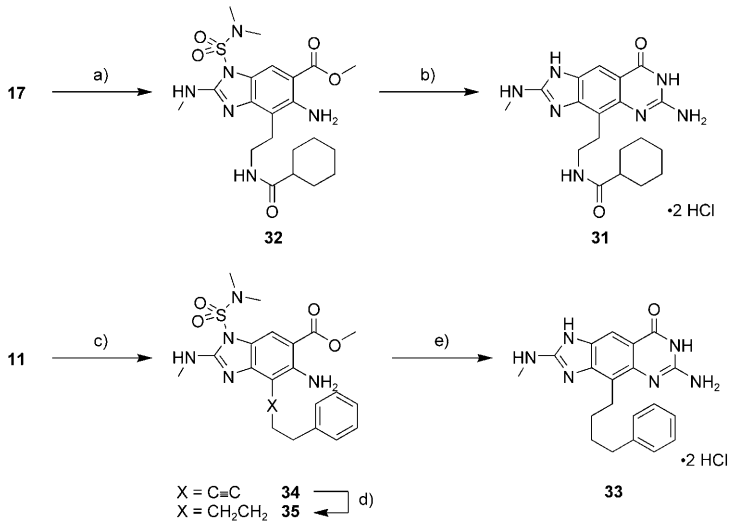

Scheme 5. Synthesis of inhibitors **31** and **33**. a) Cyclohexanecarbonyl chloride, Et_3N, CH_2Cl_2, 22 °C; 61 %. b) Chloroformamidinium chloride, dimethyl sulfone, 150 °C; 22 %. c) 4-Phenyl-1-butyne, $[PdCl_2(PPh_3)_2]$, CuI, iPr_2NH, 80 °C; 62 %. d) 1 bar H_2, Pd/C, CH_2Cl_2/MeOH, 22 °C; 77 %. e) Chloroformamidinium chloride, dimethyl sulfone, 150 °C; 54 %.

to fit the aromatic rings deeply into the hydrophobic patch.[19]

Protein–ligand co-crystal structure: The predicted binding mode of *lin*-benzoguanine **5** is further supported by a crystal structure determination, described in detail in another study.[19] The tricyclic *lin*-benzoguanine scaffold is held in position by an array of hydrogen bonds to Asp102, Asp156, Gln203, Gly230, Leu231, and Ala232, as well as by stacking interactions with the Tyr106 and Met260 sandwiching from above and below (not shown). The protonated secondary ammonium group forms two strong ionic H-bonds (d-(N···N) = 2.6 Å) to the Asp280 side chain and to a structural water molecule. The latter also has a close contact (d-(N···N) = 2.6 Å) to the (imidazole) N-atom in position 3 of the *lin*-benzoguanine scaffold. The CH_2-CH_2-NH_2^+-CH_2 unit in the linker chain shows a slightly strained *gauche* conformation in order to pick up these interactions. The cyclohexane moiety adopts a well-defined chair conformation and lies on the hydrophobic surface formed by Val45 and Leu68 (Figure 4).[19]

Table 2. *lin*-Benzoguanine inhibitors substituted in position 4 and their inhibition constants.

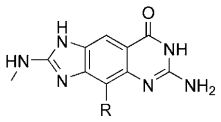

Compound	R	K_i/nM	Compound	R	K_i/nM
36	H	58 ± 36[7]	**25**	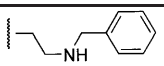	25 ± 2
33	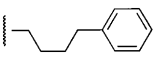	235 ± 50	**26**	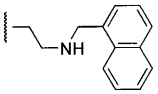	105 ± 10
15		97 ± 5	**23**	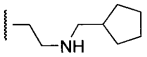	2 ± 1
18		55 ± 3	**5**	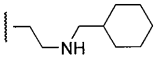	4 ± 2
27		26 ± 6	**24**	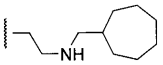	2.5 ± 1
31	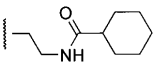	1400 ± 100			

Conclusions

In this study, the possibility of displacing fixed water molecules between Asp102 and Asp280 by polar, H-bond-forming linkers is demonstrated. While a simple alcohol, such as **15**, is unable to fully replace the function of the expelled water molecules, the amines **18** and **27** display the same or a slightly improved binding compared to the unsubstituted scaffold **36**. Accordingly, the protonated ammonium centers are able to form H-bonds strong enough to replace the ones lost by the release of water. The costs in potency associated with the desolvation of the two Asp side chains are therefore fully compensated by the formation of ionic H-bonds to Asp280 and involving a remaining water molecule in the interactions. Further substitution of the terminal ammonium group with aliphatic substituents (**23**, **5**, **24**) experiences additional hydrophobic interactions with the apolar surface of a small crevice formed by Val45 and Leu68 near the ribose-34 site, causing another favorable contribution to the binding free energy. Thus, the inhibitory constants of **23**, **5**, and **24** are further lowered and the most potent inhibitor **23**, bearing a terminal cyclopentyl ring, exhibits a K_i of 2 ± 1 nM. The aromatic substituents in inhibitors **25** and **26** seem to be too rigid for optimal nesting on molecules, in full accordance with our hypothesis. Attaching a terminal alicyclic ring to the ammonium substituent, as introduced in inhibitors **23**, **5**, and **24**, leads to a large increase in binding potency that must be due to hydrophobic interactions with the ribose-34 hydrophobic patch. Terminal aromatic rings attached to the ammonium center, as exemplified by compounds **25** and **26**, seem to be less beneficial, which is probably due to the reduced flexibility of the ring that prevents an optimal adaptation to the apolar surface crevice. Furthermore, according to the modeling, unfavorable torsional angles NH_2^+-CH_2-C_{sp2}-C_{sp2} seem to be required

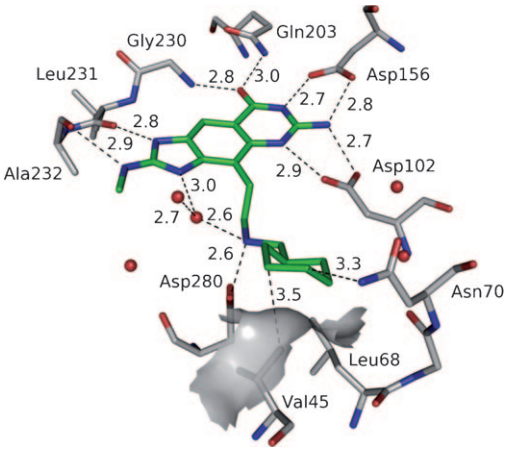

Figure 4. X-ray crystal structure of inhibitor **5** (green) in the active site of TGT from *Z. mobilis* (grey) described in ref. [19]. The residues Val45 and Leu68 form a hydrophobic surface (shown) that hosts the cyclohexane ring. Atom distances in Å. Resolution 1.78 Å. PDB code 3EOS.

the hydrophobic patch; therefore no favorable overall contribution to the binding affinity is observed.

All of these ligands, bearing different amino substituents in position 4 of the *lin*-benzoguanine scaffold, became available by a versatile synthetic route starting from the 2-methylamino-4-iodo-benzimidazole **11**. A sequence of Suzuki cross-coupling, hydroboration, Mitsunobu reaction, and Gabriel synthesis furnishes the primary amine **17** as a late common intermediate, which is further substituted *via* reductive amination. This synthetic route allows for easy further optimization of the substituent in position 4, in order to tune binding and physicochemical properties of the ligands.

Experimental Section

Materials and general methods: Compounds **7a/b** and **8** were prepared as described in the literature.[7] Details for the biological assay, the X-ray crystal structure of **28**, and the synthetic procedures for compounds **15**, **18**–**27**, and **30**–**35** can be found in the Supporting Information. Chemicals were reagent-grade, purchased from commercial suppliers, and used without further purification unless otherwise stated. AcOEt, hexane, and CH_2Cl_2 for extraction and chromatography were used in technical quality and distilled before use. Absolute THF, CH_2Cl_2, and toluene used in reactions were prepared by distillation over a drying agent (THF: Na/benzophenone; CH_2Cl_2: CaH_2; toluene: Na). Reaction monitoring was achieved by thin-layer chromatography on silica-coated glass plates with fluorescence marker (60 F_{254}, Merck). Visualization occurred by UV light (254 nm) or coloring with potassium permanganate solution ($KMnO_4$ (3 g), K_2CO_3 (20 g), NaOH (0.25 g), H_2O (300 mL)). Alternatively, analytical LC/MS using an Ultimate 3000 series LC instrument combined with an MSQ Plus mass spectrometer from Dionex, using a Zorbax Eclipse Plus C18 column (30×3 mm; 3.5 μm pore size) from Agilent or a Reprospher C18-Aqua column (30×3 mm; 3 μm pore size) from Dr. Maisch was employed. Column chromatography (CC) was done on Kieselgel 60 silica gel from Fluka or SilicaFlash F60 from SiliCycle (normal-phase), or MCI gel CHP20P from Supelco (reverse-phase) with 0–0.5 bar overpressure. The corresponding solvent mixtures are given in brackets. Drying in high vacuum (HV) was done at 10^{-2} Torr. Melting points were measured on a Büchi Meltingpoint B-540 apparatus and are uncorrected. IR spectra were recorded on a Varian 800 FT-IR ATR device equipped with a Golden-Gate ATR unit. The bands are indicated in cm^{-1} and corresponding strength (s: strong; m: medium; w: weak). Broad bands are indicated as br. NMR spectra were recorded at 22 °C unless otherwise stated. The signal positions are given in ppm relative to tetramethylsilane, the coupling constants (*J* values) in Hz. The signal multiplicities are given as s (singulet), d (doublet), t (triplet), q (quadruplet), quint. (quintet), sext. (sextet), sept. (septet), or combinations thereof. Broad signals are indicated as br. 300 MHz: Varian Gemini 300, Varian Mercury 300, or Bruker ARX 300. 400 MHz: Bruker DRX 400 or Bruker AV 400. 500 MHz: Bruker DRX 500. Mass spectra were recorded and evaluated by the MS service of the Laboratorium für Organische Chemie at ETH Zürich. Line positions are given in *m*/*z* units. EI-MS: Waters Micromass AutoSpec-Ultima spectrometer. ESI- and MALDI-MS: Varian IonSpec FT-ICR-MS spectrometer. 3-Hydroxypicolinic acid (3-HPA) was used as matrix for MALDI-MS. Elemental analyses were performed by the Mikrolabor at the Laboratorium für Organische Chemie at ETH Zürich with a LECO CHN/900 instrument. Nomenclature mainly follows the computer program ACD Name. Crystallographic pictures were prepared using PyMol.[27]

General procedure 1 (GP 1) for the cyclization with chloroformamidinium chloride:[5] The benzimidazole (1.0 equiv), chloroformamidinium chloride (2.0–2.8 equiv), and dimethylsulfone (50–67 equiv) were mixed and heated to 150 °C for 3–4 h.

General procedure 2 (GP 2) for the reductive amination of a primary amine: To the amine (1.00 equiv), a solution of the aldehyde (0.99–1.08 equiv) in CH_2Cl_2 (0.075–0.107 M) and $NaBH(OAc)_3$ (3.0–6.2 equiv) were added and the mixture was stirred at 22 °C for 30 min–17 h. Subsequently, 1 M aqueous NaOH was added and the mixture extracted with CH_2Cl_2. The combined organic phases were dried over Na_2SO_4, filtered, and evaporated. Purification was accomplished by CC (SiO_2; CH_2Cl_2/MeOH/25% aqueous NH_3 97:2:1).

Methyl 1-[(dimethylamino)sulfonyl]-2-(methylamino)-5-nitro-1*H*-benzimidazol-6-carboxylate (9): Ethanolic $MeNH_2$ solution (20 mL, 161 mmol, ~8 M) was added to **8** (3.19 g, 7.84 mmol) at 0 °C, and the mixture was stirred at the same temperature for 10 min. After evaporation, purification by CC (SiO_2; hexane/AcOEt 50:50→ 0:100) afforded **9** (2.55 g, 91%) as a yellow solid. M.p. 169–170 °C; ^{1}H NMR ($CDCl_3$, 300 MHz): δ = 7.89, 7.81 (2 s, 2H), 6.39 (br q, *J* = 4.8 Hz, 1H), 3.89 (s, 3H), 3.17 (d, *J* = 4.8 Hz, 3H), 2.95 ppm (s, 6H); ^{13}C NMR ($CDCl_3$, 75 MHz): δ = 29.95, 38.67, 53.06, 112.19, 112.94, 119.54, 133.66, 144.39, 146.33, 156.08, 165.89 ppm; IR (neat): $\tilde{\nu}$ = 3436 (m), 2923 (w), 1722 (s), 1632 (s), 1567 (m), 1524 (s), 1444 (s), 1418 (m), 1371 (s), 1343 (s), 1293 (s), 1254 (s), 1219 (s), 1149 (s), 1114 (m), 1051 (m), 1012 (m), 982 (s), 891 (m), 875 (m), 838 (m), 822 (m), 788 (m), 728 (s), 713 (m), 631 cm^{-1} (m); HR-MALDI-MS (3-HPA): *m*/*z*: calcd for $C_{12}H_{16}N_5O_6S^+$ $[M+H]^+$: 358.0816; found: 358.0822; elemental analysis calcd (%) for $C_{12}H_{15}N_5O_6S$ (357.35): C 40.33, H 4.23, N 19.60; found: C 40.62, H 4.28, N 19.42.

Methyl 5-amino-1-[(dimethylamino)sulfonyl]-2-(methylamino)-1*H*-benzimidazol-6-carboxylate (10): Compound **9** (2.55 g, 7.14 mmol) was dissolved in a mixture of AcOH/H_2O 5:1 (200 mL). Zn powder (4.72 g, 72.2 mmol) was added and the mixture stirred at 22 °C for 20 min and filtered through Celite (rinsed with MeOH). After evaporation and drying in HV, the residue was re-dissolved in CH_2Cl_2 and again filtered through Celite (rinsed with CH_2Cl_2). Purification by CC (SiO_2; AcOEt) gave **10** (2.20 g, 94%) as a pale yellow solid. M.p. 178–179 °C; ^{1}H NMR ($CDCl_3$, 300 MHz): δ = 8.00 (s, 1H), 6.62 (s, 1H), 6.33 (br q, *J* = 4.8 Hz, 1H), 5.71 (br s, 2H), 3.86 (s, 3H), 3.13 (d, *J* = 4.8 Hz, 3H), 2.91 ppm (s, 6H); ^{13}C NMR ($CDCl_3$, 75 MHz): δ = 29.75, 38.67, 51.38, 102.53, 104.28, 113.83, 123.61, 148.05, 149.24, 156.00, 168.47 ppm; IR (neat): $\tilde{\nu}$ = 3405 (s), 3306 (m), 2951 (w), 1686 (m), 1593 (s), 1452 (s), 1418 (s), 1375 (s), 1263 (s), 1236 (s), 1196 (s), 1157 (s), 1025 (s), 955 (s), 710 cm^{-1} (s); HR-MALDI-MS (3-HPA): *m*/*z*: calcd for $C_{12}H_{17}N_5O_4S^+$ $[M]^+$: 327.0996; found: 327.0989.

Methyl 5-amino-1-[(dimethylamino)sulfonyl]-4-iodo-2-(methylamino)-1*H*-benzimidazol-6-carboxylate (11): To a solution of **10** (2.20 g, 6.71 mmol) in CH_2Cl_2 (120 mL), saturated aqueous $NaHCO_3$ solution (60 mL) and iodine (2.00 g, 7.89 mmol) were added and the mixture was stirred at 22 °C for 3 d. After addition of saturated aqueous $Na_2S_2O_3$

(50 mL), the aqueous phase was extracted with CH_2Cl_2 (2×100 mL) and the combined organic phases were dried over Na_2SO_4, filtered, and evaporated. Purification by CC (SiO_2; hexane/AcOEt 50:50) yielded **11** (2.99 g, 98%) as a yellow solid. M.p. 177–178°C; ^{1}H NMR ($CDCl_3$, 300 MHz): δ=8.02 (s, 1H), 6.43 (brs, 2H), 6.38 (brq, J=5.1 Hz, 1H), 3.87 (s, 3H), 3.21 (d, J=5.1 Hz, 3H), 2.91 ppm (s, 6H); ^{13}C NMR ($CDCl_3$, 75 MHz): δ=29.91, 38.71, 51.73, 73.06, 103.85, 113.96, 121.59, 148.47, 149.88, 155.51, 167.93 ppm; IR (neat): $\tilde{\nu}$=3313 (m), 3277 (w), 2947 (w), 1683 (m), 1574 (s), 1406 (m), 1383 (s), 1261 (s), 1195 (s), 1144 (s), 1022 (s), 953 (s), 781 (m), 709 cm^{-1} (s); HR-ESI-MS: m/z: calcd for $C_{12}H_{17}IN_5O_4S^+$ $[M+H]^+$: 454.0040; found: 454.0043; elemental analysis calcd (%) for $C_{12}H_{16}IN_5O_4S$ (453.26): C 31.80, H 3.56, N 15.45; found: C 31.82, H 3.58, N 15.16.

Methyl 5-amino-1-[(dimethylamino)sulfonyl]-2-(methylamino)-4-vinyl-1*H*-benzimidazole-6-carboxylate (12): To a suspension of **11** (200 mg, 0.44 mmol) and $[PdCl_2(PPh_3)_2]$ (31 mg, 0.04 mmol) in DME (1 mL) and H_2O (0.2 mL), Et_3N (0.18 mL, 1.29 mmol) and 4,4,5,5-tetramethyl-2-vinyl-1,3,2-dioxaborolane (0.12 mL, 0.69 mmol) were added and the mixture was heated to 80°C for 75 min. After evaporation, purification by CC (SiO_2; hexane/AcOEt 67:33→50:50) provided **12** (136 mg, 87%) as a yellow oil. ^{1}H NMR ($CDCl_3$, 300 MHz): δ=7.99 (s, 1H), 6.92 (dd, J=17.9, 11.8 Hz, 1H), 6.31 (brq, J=4.9 Hz, 1H), 6.21 (dd, J=17.9, 2.1 Hz, 1H), 6.14 (brs, 2H), 5.68 (dd, J=11.8, 2.1 Hz, 1H), 3.86 (s, 3H), 3.17 (d, J=4.9 Hz, 3H), 2.90 ppm (s, 6H); ^{13}C NMR ($CDCl_3$, 75 MHz): δ=29.84, 38.74, 51.50, 104.32, 111.13, 113.20, 119.46, 123.30, 128.63, 146.12, 146.76, 155.79, 168.95 ppm; IR (neat): $\tilde{\nu}$=3418 (w), 2948 (w), 1687 (w), 1581 (s), 1406 (w), 1384 (s), 1266 (m), 1189 (s), 1159 (s), 1050 (m), 958 (m), 796 (w), 713 cm^{-1} (s); HR-MALDI-MS (3-HPA): m/z: calcd for $C_{14}H_{20}N_5O_4S^+$ $[M+H]^+$: 354.1231; found: 354.1231.

Methyl 5-amino-1-[(dimethylamino)sulfonyl]-4-(2-hydroxyethyl)-2-(methylamino)-1*H*-benzimidazole-6-carboxylate (13): Compound **12** (136 mg, 0.38 mmol) was dissolved in a 9-BBN solution (2.3 mL, 1.2 mmol; 0.5 M in THF) and stirred at 22°C for 8 h. At 0°C, H_2O_2 (0.20 mL, 1.96 mmol; 30% in H_2O) and 1 M aqueous NaOH (2.0 mL, 2.0 mmol) were carefully added. The mixture was stirred at 22°C for 40 min, diluted with saturated aqueous NH_4Cl (20 mL) and extracted with AcOEt (3×20 mL). The combined organic phases were dried over Na_2SO_4, filtered, and evaporated. Purification by CC (SiO_2; AcOEt) afforded **13** (100 mg, 70%) as a cream-colored solid. An analytical sample was obtained by recrystallization from hexane/AcOEt. M.p. 157–158°C; ^{1}H NMR ($CDCl_3$, 300 MHz): δ=7.98 (s, 1H), 6.34 (brq, J=4.9 Hz, 1H), 5.85 (brs, 2H), 4.01 (t, J=5.5 Hz, 2H), 3.85 (s, 3H), 3.12 (d, J=4.9 Hz, 3H), 2.98 (t, J=5.5 Hz, 2H), 2.92 ppm (s, 6H); ^{13}C NMR ($CDCl_3$, 75 MHz): δ=29.51, 29.87, 38.76, 51.57, 61.70, 104.85, 112.11, 112.32, 122.97, 145.90, 147.42, 155.23, 169.00 ppm; IR (neat): $\tilde{\nu}$=3427 (w), 3333 (w), 2944 (w), 1687 (w), 1592 (s), 1513 (w), 1413 (m), 1373 (m), 1267 (m), 1200 (s), 1155 (s), 1053 (m), 1024 (w), 961 (s), 790 (w), 750 (w), 712 cm^{-1} (s); HR-MALDI-MS (3-HPA): m/z: calcd for $C_{14}H_{22}N_5O_5S^+$ $[M+H]^+$: 372.1336; found: 372.1329; elemental analysis calcd (%) for $C_{14}H_{21}N_5O_5S$ (371.42): C 45.27, H 5.70, N 18.86; found: C 45.84, H 5.79, N 18.64.

Methyl 5-amino-4-{2-[(cyclohexylmethyl)amino]ethyl}-1-[(dimethylamino)sulfonyl]-2-(methylamino)-1*H*-benzimidazole-6-carboxylate (14): From **13**: Compound **13** (84 mg, 0.23 mmol) was dissolved in CH_2Cl_2 (10 mL). *p*TsCl (85 mg, 0.45 mmol), Et_3N (0.03 mL, 0.22 mmol), and DMAP (12 mg, 0.10 mmol) were added at 0°C, and the mixture was stirred at the same temperature for 3.5 h and evaporated. CC (SiO_2; hexane/AcOEt 50:50) afforded a colorless oil (71 mg), which was dissolved in CH_2Cl_2 (10 mL). At 0°C, (cyclohexylmethyl)amine (0.20 mL, 1.54 mmol) was added, the mixture allowed to reach 22°C during 26 h, and the solvent removed by evaporation. Purification by CC (SiO_2; CH_2Cl_2/MeOH/25% aqueous NH_3 97:2:1) gave **14** (40 mg, 38%) as a white solid. From **17**: GP 2 using **17** (21.9 mg, 0.059 mmol) and cyclohexanecarbaldehyde (6.5 mg, 0.058 mmol) yielded **14** (16.9 mg, 61%) as a white solid. M.p. 173–174°C; ^{1}H NMR ($CDCl_3$, 400 MHz): δ=7.92 (s, 1H), 6.24 (q, J=4.9 Hz, 1H), 3.84 (s, 3H), 3.13 (d, J=4.9 Hz, 3H), 3.03 (t, J=6.4 Hz, 2H), 2.89 (s, 6H), 2.88 (t, J=6.4 Hz, 2H), 2.47 (d, J=6.7 Hz, 2H), 1.72–1.66 (m, 5H), 1.47–1.37 (m, 1H), 1.27–1.07 (m, 3H), 0.93–0.83 ppm (m, 2H); ^{13}C NMR ($CDCl_3$, 100 MHz): δ=26.09, 26.27, 26.68, 29.84, 31.47, 38.13, 38.76, 49.12, 51.41, 56.82, 104.35, 111.98, 113.48, 122.91, 146.98, 148.18, 155.37, 169.16 ppm; IR (neat): $\tilde{\nu}$=3437 (w), 3413 (w), 3338 (w), 2926 (w), 2842 (w), 1676 (w), 1583 (s), 1505 (w), 1415 (s), 1389 (m), 1312 (w), 1262 (m), 1202 (s), 1161 (s), 1074 (w), 1021 (w), 962 (m), 891 (w), 807 (w), 715 (s), 662 cm^{-1} (w); HR-MALDI-MS (3-HPA): m/z: calcd for $C_{21}H_{35}N_6O_4S^+$ $[M+H]^+$: 467.2435; found: 467.2439.

6-Amino-4-{2-[(cyclohexylmethyl)amino]ethyl}-2-(methylamino)-1,7-dihydro-8*H*-imidazo[4,5-*g*]quinazolin-8-one (5): GP 1 was followed using **14** (38 mg, 0.081 mmol). Purification by CC (MCI gel; H_2O[0.1% HCl]/MeCN 100:0→95:5), followed by lyophilization, provided **5** (21 mg, 54%, HCl triple salt) as a fawn solid. M.p. > 250°C; ^{1}H NMR (D_2O + 1 drop trifluoroacetic acid (TFA), 400 MHz): δ=7.91 (s, 1H), 3.40–3.36 (m, 2H), 3.28–3.23 (m, 2H), 3.10 (s, 3H), 2.95 (d, J=6.4 Hz, 2H), 1.72–1.66 (m, 5H), 1.60 (brd, J=12.0 Hz, 1H), 1.26–1.10 (m, 3H), 1.02–0.94 ppm (m, 2H); ^{13}C NMR (D_2O + 1 drop TFA, 100 MHz): δ=22.01, 24.92, 25.43, 29.18, 29.82, 34.66, 45.65, 54.06, 107.02, 108.70, 111.71, 128.05, 133.54, 136.09, 150.98, 153.07, 161.23 ppm; IR (neat): $\tilde{\nu}$=2924 (m), 2847 (w), 2797 (brw), 1675 (s), 1645 (s), 1529 (w), 1444 (s), 1310 (w), 1227 (w), 1153 (w), 1097 (w), 982 (m), 832 (w), 756 cm^{-1} (w); HR-ESI-MS: m/z: calcd for $C_{19}H_{28}N_7O^+$ $[M+H]^+$: 370.2350; found: 370.2352.

Methyl 5-amino-1-[(dimethylamino)sulfonyl]-4-[2-(1,3-dioxo-1,3-dihydro-2*H*-isoindol-2-yl)ethyl]-2-(methylamino)-1*H*-benzimidazole-6-carboxylate (16): To a solution of **13** (374 mg, 1.01 mmol) in CH_2Cl_2 (10 mL), PPh_3 (538 mg, 2.05 mmol), DIAD (0.40 mL, 2.03 mmol), and phthalimide (299 mg, 2.03 mmol) were added and the mixture was stirred at 22°C for 16 h and evaporated. Purification by CC (SiO_2; hexane/AcOEt 67:33→50:50) gave **16** (429 mg, 85%) as a yellow solid. M.p. 206–209°C; ^{1}H NMR ($CDCl_3$, 300 MHz): δ=7.96 (s, 1H), 7.81, 7.71 (AA′MM′, 4H), 6.27 (brs, 2H), 6.16 (brq, J=4.9 Hz, 1H), 3.93 (dd, J=8.4, 6.7 Hz, 2H), 3.85 (s, 3H), 3.20 (dd, J=8.4, 6.7 Hz, 2H), 3.03 (d, J=4.9 Hz, 3H), 2.85 ppm (s, 6H); ^{13}C NMR ($CDCl_3$, 100 MHz): δ=24.23, 29.68, 35.78, 38.77, 51.44, 104.23, 109.57, 112.78, 122.79, 123.11, 132.33, 133.79, 147.37, 147.44, 155.60, 168.41, 169.05 ppm; IR (neat): $\tilde{\nu}$=3466 (w), 3426 (w), 3362 (w), 2944 (w), 1763 (w), 1703 (m), 1673 (w), 1584 (s), 1428 (w), 1394 (m), 1274 (m), 1206 (s), 1157 (s), 1103 (w), 1066 (m), 965 (m), 792 (w), 716 cm^{-1} (s); HR-MALDI-MS (3-HPA): m/z: calcd for $C_{22}H_{25}N_6O_6S^+$ $[M+H]^+$: 501.1551; found: 501.1546.

Methyl 5-amino-4-(2-aminoethyl)-1-[(dimethylamino)sulfonyl]-2-(methylamino)-1*H*-benzimidazole-6-carboxylate (17): To a solution of **16** (458 mg, 0.92 mmol) in CH_2Cl_2 (10 mL) and MeOH (10 mL), hydrazine monohydrate (0.45 mL, 9.3 mmol) was added and the mixture stirred at 22°C for 2 d. After evaporation, the mixture was taken up in 1 M aqueous NaOH (50 mL) and extracted with CH_2Cl_2 (4×50 mL). The combined organic phases were dried over Na_2SO_4, filtered, and evaporated to yield **17** (327 mg, 96%) as a yellow solid. No further purification was done. M.p. 139–141°C; ^{1}H NMR ($CDCl_3$, 300 MHz): δ=7.92 (s, 1H), 6.25 (brq, J=4.8 Hz, 1H), 3.83 (s, 3H), 3.11 (d, J=4.8 Hz, 3H), 2.99 (brs, 4H), 2.88 ppm (s, 6H); ^{13}C NMR ($CDCl_3$, 100 MHz): δ=29.24, 29.79, 38.67, 40.83, 51.38, 104.43, 112.05, 112.22, 122.99, 147.22, 147.53, 155.40, 169.04 ppm; IR (neat): $\tilde{\nu}$=3466 (w), 3428 (w), 3362 (w), 2944 (w), 1763 (w), 1703 (w), 1672 (w), 1582 (s), 1427 (w), 1394 (m), 1271 (m), 1204 (s), 1157 (s), 1102 (w), 963 (m), 791 (m), 710 cm^{-1} (s); HR-MALDI-MS (3-HPA): m/z: calcd for $C_{14}H_{23}N_6O_4S^+$ $[M+H]^+$: 371.1496; found: 371.1501.

Methyl 8-benzyl-3-[(dimethylamino)sulfonyl]-2-(methylamino)-3,6,7,8,9,10-hexahydroimidazo[4,5-*g*][1,3]benzodiazepine-5-carboxylate (28) and methyl 5-amino-4-{2-[benzyl(methyl)amino]ethyl}-1-[(dimethylamino)sulfonyl]-2-(methylamino)-1*H*-benzimidazole-6-carboxylate (29): A solution of **21** (63 mg, 0.137 mmol) in CH_2Cl_2 (2.0 mL) was cooled to 0°C, and formic acid (16 μL, 0.42 mmol) and a solution of formaldehyde (13.5 μL, 0.175 mmol; 36% in H_2O) in H_2O (0.1 mL) were added. The mixture was allowed to warm to 22°C during 16 h, 1 M aqueous NaOH (10 mL) was added, and the mixture was extracted with CH_2Cl_2 (2×10 mL). The combined organic phases were dried over Na_2SO_4, filtered, and evaporated, providing **28** as a pale yellow solid. M.p. 156–158°C; ^{1}H NMR ($CDCl_3$, 300 MHz): δ=7.97 (s, 1H), 7.73 (brt, J=4.0 Hz, 1H), 7.44–7.25 (m, 5H), 6.27 (q, J=4.9 Hz, 1H), 4.16 (d, J=4.0 Hz, 2H), 3.95 (s, 2H), 3.84 (s, 3H), 3.39–3.35 (m, 2H), 3.15 (d, J=4.9 Hz, 3H), 3.10–3.07 (m, 2H), 2.90 ppm (s, 6H); ^{13}C NMR ($CDCl_3$, 100 MHz): δ=25.36,

29.83, 38.75, 51.63, 52.04, 56.02, 65.38, 107.35, 111.93, 118.19, 124.16, 127.11, 128.38, 129.39, 138.62, 147.18, 152.42, 155.25, 169.23 ppm; IR (neat): $\tilde{\nu}$ = 3409 (w), 3320 (w), 2937 (w), 2919 (w), 1681 (w), 1635 (w), 1573 (s), 1427 (m), 1410 (m), 1372 (s), 1354 (s), 1271 (m), 1198 (s), 1133 (s), 1049 (s), 1006 (s), 971 (w), 794 (m), 738 (s), 712 cm^{-1} (s); HR-MALDI-MS (3-HPA): *m*/*z*: calcd for $C_{22}H_{29}N_6O_4S^+$ $[M+H]^+$: 473.1966; found: 473.1966. The crude intermediate was dissolved in 1,2-dichloroethane (2.0 mL), $NaBH(OAc)_3$ (161 mg, 0.76 mmol) was added, and the mixture heated to reflux for 30 min. Subsequently, 1 M aqueous NaOH (10 mL) was added and the mixture extracted with CH_2Cl_2 (2×10 mL). The combined organic phases were dried over Na_2SO_4, filtered, and evaporated. Purification by CC (SiO_2; CH_2Cl_2/MeOH/25% aqueous NH_3 97:2:1) afforded **29** (54 mg, 83%) as a colorless oil. ^{1}H NMR ($CDCl_3$, 300 MHz): δ = 7.93 (s, 1H), 7.34–7.20 (m, 5H), 6.56 (br s, 2H), 6.24 (q, *J* = 4.9 Hz, 1H), 3.85 (s, 3H), 3.62 (s, 2H), 3.12 (d, *J* = 4.9 Hz, 3H), 3.10 (t, *J* = 6.6 Hz, 2H), 2.89 (s, 6H), 2.69 (t, *J* = 6.6 Hz, 2H), 2.30 ppm (s, 3H); ^{13}C NMR ($CDCl_3$, 100 MHz): δ = 23.90, 29.79, 38.75, 42.21, 51.38, 56.52, 62.22, 104.27, 111.89, 113.81, 122.89, 127.03, 128.23, 129.12, 138.66, 146.82, 148.18, 155.35, 169.17 ppm; IR (neat): $\tilde{\nu}$ = 3417 (w), 2946 (w), 2840 (w), 2794 (w), 1682 (w), 1638 (w), 1582 (s), 1413 (m), 1392 (m), 1373 (w), 1272 (m), 1202 (s), 1156 (s), 1067 (w), 962 (m), 908 (w), 793 (w), 733 (m), 715 cm^{-1} (s); HR-MALDI-MS (3-HPA): *m*/*z*: calcd for $C_{22}H_{31}N_6O_4S^+$ $[M+H]^+$: 475.2122; found: 475.2121.

Acknowledgements

We are grateful to the ETH Research Council and F. Hoffmann-La Roche for financial support. We thankfully acknowledge the support for the work at the Philipps-University, Marburg by the Deutsche Forschungsgemeinschaft (Grants KL1204/1-3 and KL1204/9-1) and the Graduiertenkolleg ("Protein function at the atomic level", G. Klebe, University of Marburg).

[1] N. Okada, C. Sasakawa, T. Tobe, M. Yamada, S. Nagai, K. A. Talukder, K. Komatsu, S. Kanegasaki, M. Yoshikawa, *Mol. Microbiol.* **1991**, *5*, 187–195.
[2] K. L. Kotloff, J. P. Winickoff, B. Ivanoff, J. D. Clemens, D. L. Swerdlow, P. J. Sansonetti, G. K. Adak, M. M. Levine, *WHO Bull.* **1999**, *77*, 651–666.
[3] D. Iwata-Reuyl, *Bioorg. Chem.* **2003**, *31*, 24–43.
[4] G. E. Keyser, N. J. Leonard, *J. Org. Chem.* **1976**, *41*, 3529–3532.
[5] E. A. Meyer, N. Donati, M. Guillot, W. B. Schweizer, F. Diederich, B. Stengl, R. Brenk, K. Reuter, G. Klebe, *Helv. Chim. Acta* **2006**, *89*, 573–597.
[6] B. Stengl, E. A. Meyer, A. Heine, R. Brenk, F. Diederich, G. Klebe, *J. Mol. Biol.* **2007**, *370*, 492–511.
[7] S. R. Hörtner, T. Ritschel, B. Stengl, C. Kramer, W. B. Schweizer, B. Wagner, M. Kansy, G. Klebe, F. Diederich, *Angew. Chem.* **2007**, *119*, 8414–8417; *Angew. Chem. Int. Ed.* **2007**, *46*, 8266–8269.
[8] T. Ritschel, S. Hoertner, A. Heine, F. Diederich, G. Klebe, *ChemBioChem* **2009**, *10*, 716–727.
[9] J. E. Ladbury, *Chem. Biol.* **1996**, *3*, 973–980.
[10] F. A. Quiocho, D. K. Wilson, N. K. Vyas, *Nature* **1989**, *340*, 404–407.
[11] P. Y. S. Lam, P. K. Jadhav, C. J. Eyermann, C. N. Hodge, Y. Ru, L. T. Bacheler, J. L. Meek, M. J. Otto, M. M. Rayner, Y. N. Wong, C.-H. Chang, P. C. Weber, D. A. Jackson, T. R. Sharpe, S. Erickson-Viitanen, *Science* **1994**, *263*, 380–384.
[12] J. R. H. Tame, G. N. Murshudov, E. J. Dodson, T. K. Neil, G. G. Dodson, C. F. Higgins, A. J. Wilkinson, *Science* **1994**, *264*, 1578–1581.
[13] M. L. Verdonk, G. Chessari, J. C. Cole, M. J. Hartshorn, C. W. Murray, J. W. M. Nissink, R. D. Taylor, R. Taylor, *J. Med. Chem.* **2005**, *48*, 6504–6515.
[14] C. Barillari, J. Taylor, R. Viner, J. W. Essex, *J. Am. Chem. Soc.* **2007**, *129*, 2577–2587.
[15] A. Amadasi, J. A. Surface, F. Spyrakis, P. Cozzini, A. Mozzarelli, G. E. Kellogg, *J. Med. Chem.* **2008**, *51*, 1063–1067.
[16] J. D. Dunitz, *Science* **1994**, *264*, 670.
[17] J. D. Dunitz, *Chem. Biol.* **1995**, *2*, 709–712.
[18] J. Günther, A. Bergner, M. Hendlich, G. Klebe, *J. Mol. Biol.* **2003**, *326*, 621–636.
[19] T. Ritschel, P. C. Kohler, G. Neudert, A. Heine, F. Diederich, G. Klebe, *ChemMedChem*, DOI: 10.1002/cmdc.200900343.
[20] P. R. Gerber, K. Müller, *J. Comput.-Aided Mol. Des.* **1995**, *9*, 251–268.
[21] X. Zhang, Y. Zhang, J. Huang, R. P. Hsung, K. C. M. Kurtz, J. Oppenheimer, M. E. Petersen, I. K. Sagamanova, L. Shen, M. R. Tracey, *J. Org. Chem.* **2006**, *71*, 4170–4177.
[22] O. Hromatka, M. Knollmüller, H. Deschler, *Monatsh. Chem.* **1969**, *100*, 469–478.
[23] P. G. Gassman, S. J. Lee, *J. Org. Chem.* **1986**, *51*, 267–268.
[24] J. M. Gardiner, M. R. Bryce, P. A. Bates, M. B. Hursthouse, *J. Org. Chem.* **1990**, *55*, 1261–1266.
[25] H. M. Ma, Z. Z. Liu, S. Z. Chen, X. T. Liang, *Chin. Chem. Lett.* **2004**, *15*, 759–761.
[26] G. DeStevens, M. Dughi, *J. Am. Chem. Soc.* **1961**, *83*, 3087–3091.
[27] W. DeLano, **2006**, http://www.pymol.org.

Received: May 13, 2009
Published online: September 10, 2009

